

# Isolation and Characterization of Elusive Tetrabenzylthorium Complexes

D. M. Ramitha Y. P. Rupasinghe, Makayla R. Baxter, Matthias Zeller, and Suzanne C. Bart\*



Cite This: *Organometallics* 2023, 42, 2079–2086



Read Online

## ACCESS |

Metrics & More

Article Recommendations

Supporting Information

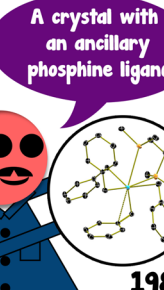
**ABSTRACT:** The synthesis and crystal structure of homoleptic tetrabenzylthorium,  $\text{Th}(\text{Bn})_4$  (4) ( $\text{Bn}$  = benzyl,  $\text{CH}_2\text{Ph}$ ), is presented herein. First reported by Thiele and co-workers 48 years ago, the characterization of  $\text{Th}(\text{Bn})_4$  was limited due to the material's sensitivity. Several other new tetrabenzyl complexes were also crystallographically isolated and discussed here, including  $\text{Th}(\text{Bn})_4(\text{THF})_2$  (1-THF) and  $\text{Th}(\text{Bn})_4(\text{dme})$  (2-dme, dme = 1,2-dimethoxyethane). A previously isolated phosphine adduct of tetrabenzylthorium,  $\text{Th}(\text{Bn})_4(\text{dmpe})$  (3-dmpe, dmpe = 1,2-bis(dimethylphosphino)ethane), is reported with a modified synthesis and updated structural data. A short discussion of hapticity and coordination modes of actinide benzyl ligands is also presented. Studies on the utility of 4 as a synthon to other organothorium compounds are reported, including  $\text{Th}(\text{adap})_2(\text{pyr})_3$  (5-ap) (pyr = pyridine), formed from the reaction of 4 with 2-(adamantan-2-ylamino)-4,6-di-*tert*-butylphenol ( $\text{H}_2\text{adap}$ ). All compounds were characterized by multinuclear NMR spectroscopy and X-ray crystallography.

Merseburg, Germany



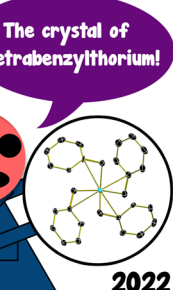
1974

California, USA



1983

Indiana, USA



2022

## INTRODUCTION

Inquiries into uranium isotopic separation during the Manhattan Project era created a desire for volatile uranium complexes for centrifugal separation.<sup>1</sup> Gilman and co-workers attempted syntheses of homoleptic tetravalent uranium 1,3-dicarbonyl chelates, but due to temperature sensitivity and an undesired high molecular weight, further uranium alkyl work was suspended.<sup>1</sup> About two decades later in 1974, Thiele and co-workers introduced tetrabenzyluranium and thorium complexes, producing reliable syntheses without the necessity of an ancillary ligand.<sup>2,3</sup> Though this work suggested multidentate coordination of the benzyl ligand, both the  $\text{U}(\text{Bn})_4[\text{MgCl}_2]$  and  $\text{Th}(\text{Bn})_4$  ( $\text{Bn}$  = benzyl,  $\text{CH}_2\text{Ph}$ ) were accompanied by limited characterization due to temperature and air sensitivity.<sup>2,3</sup> Given the advancements in glovebox technology over the past decades, various benzyl actinide derivatives were synthesized and reported, including structural characterization.<sup>4–8</sup> However, most structures isolated with uranium and thorium used ancillary organic ligands as supports.<sup>4</sup> Progress in isolating unsupported alkyl complexes has been slow, with most complexes being isolated in the last two decades.<sup>4,5,9,10</sup>

In 1984, structural characterization of tetrabenzylthorium was achieved with the addition of a stabilizing phosphine ligand, producing  $\text{Th}(\text{Bn})_4(\text{dmpe})$  (dmpe = 1,2-bis(dimethylphosphino)ethane).<sup>11</sup> The synthesis of this complex was achieved via the addition of benzyl lithium to  $\text{ThCl}_4(\text{dmpe})$  at  $-70^\circ\text{C}$ .<sup>11</sup> In the same year, the first

homoleptic thorium alkyl complex,  $[\text{Li}(\text{TMEDA})_3[\text{Th}(\text{Me})_7]]$ , was reported with structural characterization depicting a monocapped trigonal prismatic geometry.<sup>12</sup> This differs from the analogous uranium complex, as uranium adopts a six-coordinate geometry with  $[\text{Li}(\text{TMEDA})_2[\text{U}(\text{Me})_6]]$ , likely due to its smaller ionic radius.<sup>9</sup> Hayton, Walensky, and co-workers reported multiple homoleptic thorium alkyls, including  $[\text{K}(\text{THF})_2[\text{Th}(\text{Bn})_6]]$ .<sup>5</sup> Despite these advancements, the true molecular structure of tetrabenzylthorium without an ancillary ligand has been elusive.

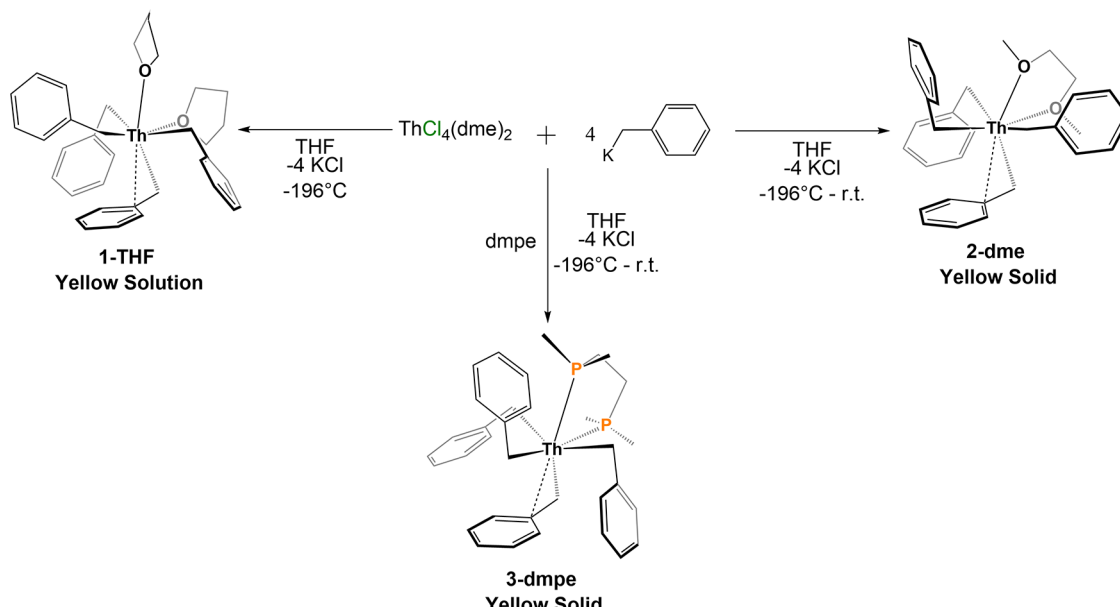
Tetrabenzylthorium derivatives are of interest for advancing studies related to actinide catalysis, including polymerization, as similar chemistry has been noted for Group IV metals.<sup>13–16</sup> Such species are also potential starting materials to generate more highly decorated compounds bearing anionic ligands *via* protonation, as the toluene byproduct is easy to remove *in vacuo*. The molecular structures of tetrabenzylhafnium, tetrabenzylzirconium, and tetrabenzyltitanium have all been established crystallographically, and their reactivity was subsequently explored.<sup>14,15</sup> Of particular interest has been

Received: May 23, 2023

Published: August 2, 2023



Scheme 1. Synthesis of 1-THF, 2-dme, and 3-dmpe



understanding the hapticity of the benzyl groups in tetrabenzylzirconium;<sup>17,18</sup> however, studies of similar rigor are lacking for tetrabenzylthorium and related complexes, with the only example being that from Andersen, Zalkin, and co-workers who studied  $\text{Th}(\text{Bn})_4(\text{dmpe})$ .<sup>11</sup>

Inspired by these studies and by our own reported ancillary ligand-free tetrabenzyluranium derivatives,<sup>4</sup> we explored the synthesis and characterization of parent tetrabenzylthorium,  $\text{Th}(\text{Bn})_4$  (4), and several related complexes with Lewis bases, including  $\text{Th}(\text{Bn})_4(\text{THF})_2$  (**1-THF**),  $\text{Th}(\text{Bn})_4(\text{dme})$  (**2-dme**, dme = 1,2-dimethoxyethane), and  $\text{Th}(\text{Bn})_4(\text{dmpe})$  (**3-dmpe**). These complexes, along with their respective spectroscopic and structural data, as well as preliminary reactivity studies of these derivatives as synthons for organothorium complexes, are reported.

## ■ RESULTS AND DISCUSSION

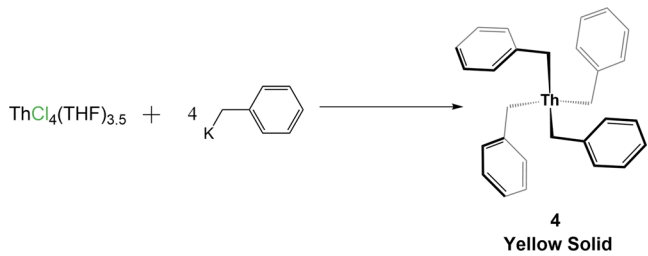
**Synthesis of Tetrabenzylthorium Compounds.** Initial attempts at the synthesis of the tetrabenzylthorium family followed the analogous synthesis of tetrabenzyluranium, which involved mixing thawing solutions of  $\text{UCl}_4$  and 4 equiv of benzylpotassium ( $\text{KBn}$ ).<sup>4</sup> However, with  $\text{ThCl}_4(\text{dme})_2$ , the solution had inconsistent color changes, such as turning orange-yellow, compared to the expected yellow as indicated by Thiele and co-workers.<sup>2</sup> Addition of  $\text{KBn}$  in two portions circumvented this issue, and the observed color was consistently yellow. It is important to note that even a slight excess of  $\text{KBn}$  needs to be avoided, as this causes the solution to turn orange, indicating the possible formation of the hexabenzylthorium dianion along with the desired tetrabenzylthorium.<sup>5</sup> Hence, a THF solution of exactly 4 equiv of  $\text{KBn}$  was added in two portions to a thawing THF solution of  $\text{ThCl}_4(\text{dme})_2$  under light-free conditions (Scheme 1). Immediate workup at room temperature resulted in intractable decomposition products and a mixture of  $\text{Th}(\text{Bn})_4(\text{THF})_2$  (**1-THF**) and  $\text{Th}(\text{Bn})_4(\text{dme})$  (**2-dme**) as indicated by  $^1\text{H}$  NMR spectroscopy (Figure S1). However, workup at  $-10^\circ\text{C}$  resulted in the isolation of **2-dme** in moderate yield (56%). The  $^1\text{H}$  NMR spectrum showed six resonances with four of

those assigned to equivalent benzyl group protons and two assigned to dme protons (Figure S2). The  $^{13}\text{C}$  NMR spectrum revealed five resonances assigned to the equivalent benzyl group carbons and two to the dme carbons (Figure S3). Compound **1-THF** could not be isolated as a fine powder but could be isolated as crystals by immediate filtration of a THF solution of the reaction followed by slow addition of cold pentane over several days with a yield of 74% when dried under *vacuo*. If the THF solution is left at room temperature, decomposition is observed within minutes, which is consistent with observations by Thiele and co-workers.<sup>2</sup>

In order to compare the features of **1-THF** and **2-dme**, previously reported  $\text{Th}(\text{Bn})_4(\text{dmpe})$  (**3-dmpe**) was synthesized using a similar procedure as **2-dme**, followed by the addition of a thawing THF solution of dmpe. This procedure is different from the previous method reported by Andersen, Zalkin, and co-workers as the starting material used was the dme adduct,  $\text{Th}(\text{Bn})_4(\text{dme})_2$ , in THF compared to using the THF adduct,  $\text{Th}(\text{Bn})_4(\text{THF})_{3.5}$ , in diethyl ether.<sup>11</sup> Workup done at room temperature afforded a bright yellow solid in high yield (81%, Scheme 1). The  $^1\text{H}$  NMR spectrum of **3-dmpe** displayed several resonances assignable to the benzyl groups and two resonances assignable to the dmpe group (Figure S4).  $^{31}\text{P}$  NMR spectroscopy indicated a single resonance at  $-26.16\text{ ppm}$  assigned to the dmpe ligand (Figure S5). The  $^{13}\text{C}$  NMR spectrum revealed five resonances assigned to the equivalent benzyl group carbons and two to the dmpe ligand carbons (Figure S6).

Given that **2-dme** is obtained exclusively when  $\text{ThCl}_4(\text{dme})_2$  is used and the workup is done at  $-10^\circ\text{C}$ , another starting material was necessary to obtain a homoleptic tetrabenzyl complex without ancillary ligands. As such,  $\text{ThCl}_4(\text{THF})_{3.5}$  was used because Thiele and co-workers confirmed the isolation of  $\text{Th}(\text{Bn})_4$  via elemental analysis and  $^1\text{H}$  NMR spectroscopy using this starting material.<sup>2</sup> Addition of a thawing solution of 4 equiv of  $\text{KBn}$  to a thawing solution of  $\text{ThCl}_4(\text{THF})_{3.5}$  resulted in  $\text{Th}(\text{Bn})_4$  (4) after workup at  $-10^\circ\text{C}$  in 77% yield (Scheme 2). The  $^1\text{H}$  NMR spectrum of **4** revealed four resonances assigned to equivalent benzyl groups (Figure S7)

Scheme 2. Synthesis of 4



and the  $^{13}\text{C}$  NMR spectrum of 4 revealed five resonances assigned to equivalent benzyl groups in solution (Figure S8).

#### Crystallography of Tetrabenzylthorium Complexes.

Yellow rod-shaped crystals of 1-THF suitable for single-crystal X-ray diffraction were generated by adding pentane dropwise over several days to a freshly filtered THF reaction mixture at  $-35^\circ\text{C}$  (Figures 1 and S12). Crystals of 2-dme and 3-dmpe were both grown from a concentrated solution of toluene as yellow rods at  $-35^\circ\text{C}$  (Figures 1 and S12). Finally, suitable crystals of 4 were obtained either from concentrated toluene at  $-35^\circ\text{C}$  ( $4\text{-}\eta^4$ ) or by layering a pentane solution of 4 with cyclopentane at  $-35^\circ\text{C}$  ( $4\text{-}\eta^3$ ) (Figures 1 and S12).

Refinement of the data showed that compounds 1-THF and 3-dmpe both crystallize in the  $P\bar{1}$  space group and have one molecule in the asymmetric unit. Despite being grown in the same manner, 3-dmpe (from the original work by Andersen, Zalkin, and co-workers) was reported to have two molecules in the asymmetric unit.<sup>11</sup> Compound 2-dme crystallizes in the monoclinic  $P21/c$  space group with two molecules in its asymmetric unit. Data collection for crystals of 4 at  $150\text{ K}$

using either method (toluene or pentane/cyclopentane) showed crystallization in the  $P21/c$  space group; the toluene crystal had only one molecule in the asymmetric unit, whereas the pentane/cyclopentane crystals had two. During measurement of the pentane/cyclopentane crystals of 4, it was found that the crystal underwent a phase transition from  $Pccn$  to  $P21/c$  upon cooling below  $175\text{ K}$ . The phase change involves a change of one of the  $90^\circ$  angles to nearly  $91^\circ$  (at  $150\text{ K}$ ) and loss of orthorhombic symmetry. After the phase transition, the crystal is twinned by the previous orthorhombic symmetry, and reflections split at medium and high angles. The phase transition is reversible under retention of the single crystal if warmed back up above  $175\text{ K}$  slowly. Interestingly, crystal data collected at  $190\text{ K}$  also had one molecule in the asymmetric unit compared to two molecules at  $150\text{ K}$ .

Based on the quality of the crystals, reliable structural parameters to understand the coordination environment of the thorium center could be obtained (Table 1). The Th–C bond lengths for the methylene carbons for the entire family of compounds, 1-THF, 2-dme, 3-dmpe,  $4\text{-}\eta^3$ , and  $4\text{-}\eta^4$ , were found to range from  $2.506(16)$  to  $2.583(6)$  Å and are consistent with previously reported benzylthorium methylene carbon distances ( $2.491$ – $2.687$  Å).<sup>5,19–24</sup>

In the cases of 1-THF, 2-dme, and 3-dmpe, where ancillary ligands are present, the geometries of the thorium ions can be described as distorted octahedra with the Th–O/Th–P bonds *trans* to the benzyl groups. The complexes of 4 are best described as distorted tetrahedra if only the anionic Th–C bonds are considered. Despite the difference in coordination sphere compared to 4, 1-THF, 2-dme, and 3-dmpe have Th–

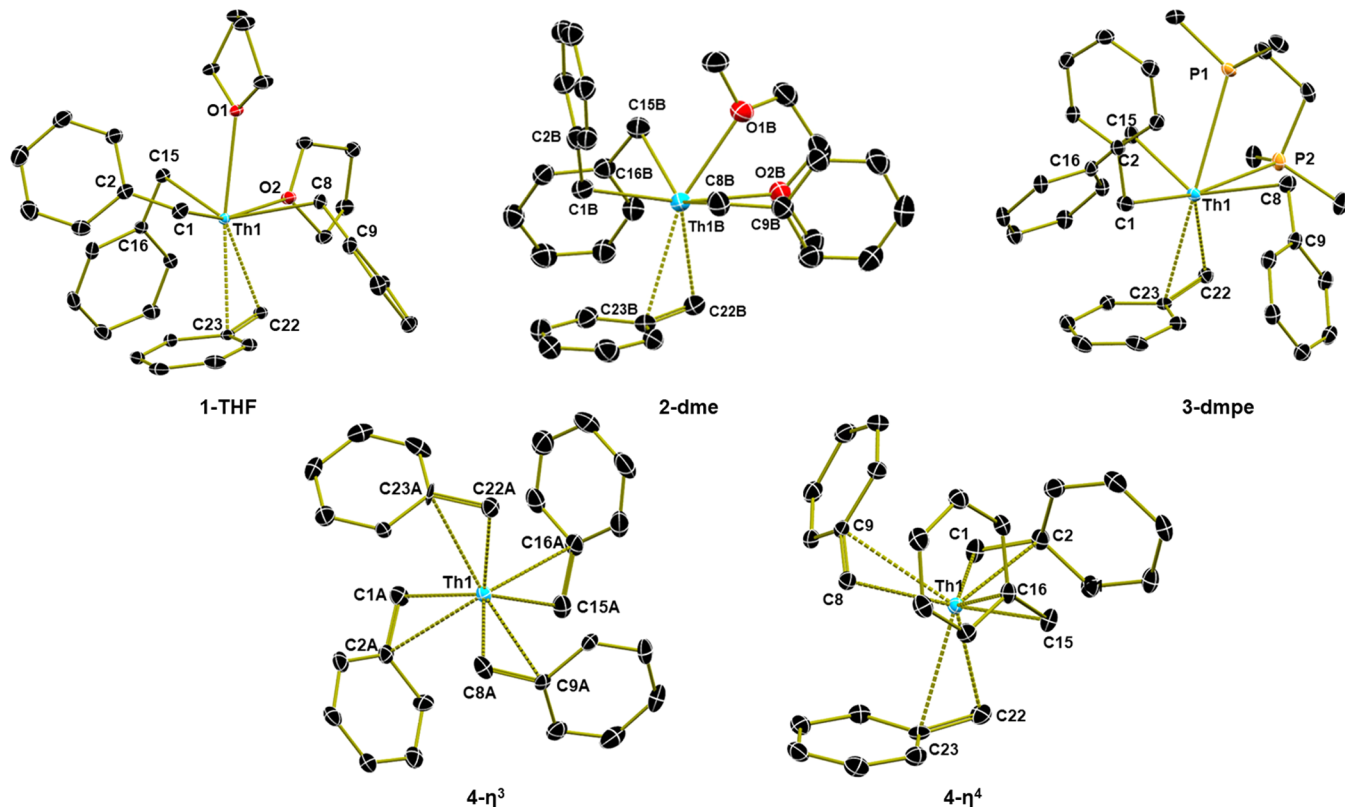


Figure 1. Molecular structures shown with 30% probability ellipsoids. Top: 1-THF, 2-dme, and 3-dmpe. Bottom:  $4\text{-}\eta^3$  (grown from pentane/cyclopentane) and  $4\text{-}\eta^4$  (grown from toluene). Hydrogen atoms, co-crystallized solvent molecules, and additional bonds are omitted for clarity.

Table 1. Bond Lengths of Tetrabenzylthorium Compounds in Å

	1-THF	2-dme A	2-dme B	3-dmpe
Th1-C1	2.5641 (16)	2.561 (6)	2.544 (6)	2.5568 (16)
Th1-C8	2.5455 (18)	2.538 (6)	2.527 (7)	2.579 (2)
Th1-C15	2.5656 (18)	2.525 (7)	2.555 (6)	2.5685 (18)
Th1-C22	2.5498 (16)	2.583 (6)	2.554 (5)	2.5231 (16)
average	2.556	2.552	2.545	2.557
	4- $\eta^4$	4- $\eta^3$ (190 K)	4- $\eta^3$ (150 K) A	4- $\eta^3$ (150 K) B
Th1-C1	2.5641 (16)	2.525 (3)	2.524 (15)	2.506 (16)
Th1-C8	2.5455 (18)	2.514 (3)	2.513 (16)	2.508 (16)
Th1-C15	2.5656 (18)	2.514 (3)	2.529 (17)	2.532 (14)
Th1-C22	2.5498 (16)	2.519 (3)	2.520 (16)	2.526 (18)
average	2.5563	2.518	2.522	2.518

C bond distances that are only slightly longer than these homoleptic species.

**Hapticity of Tetrabenzyl Compounds.** In addition to the anionic Th–methylene carbon linkages in these species, the hapticity of the benzyl groups must also be considered for a complete bonding picture. The hapticity describes instances where ligands containing extended  $\pi$ -systems have covalent bonding interactions to the metal ion.<sup>25</sup> Because the *f* elements have larger coordination spheres compared to their transition-metal counterparts, the hapticity of their benzyl groups is generally greater than  $\eta^1$ . Each benzyl group must be considered separately, and the hapticity is generally assigned based on crystallographic parameters or computational studies, depending on interactions of the phenyl  $\pi$ -system with the *f*-element ion.

To effectively describe benzyl group hapticity, various models have been developed for both *d*- and *f*-block organometallics. In the case of transition metals, Parkin describes the hapticity of Group IV tetrabenzyl complexes, which are often considered smaller analogues of thorium, for two polymorphs of tetrabenzylzirconium.<sup>16</sup> Lanthanide tribenzyl complexes have been classified by Liddle, where again, ligand hapticity was assigned using crystallographic parameters.<sup>26</sup> In the family  $[\text{Ln}(\text{Bz})_3(\text{THF})_3]$  ( $\text{Ln} = \text{Ce, Pr, Nd, Sm, Gd, Dy, Er}$ ), these ions were found to be *fac*-octahedral, with their hapticities varying as determined by van der Waals radii. Cerium, praseodymium, neodymium, and lanthanum were found to contain 3  $\eta^2$ -benzyl groups, whereas samarium showed only one  $\eta^2$  interaction, and yttrium, gadolinium, dysprosium, and erbium showed none. For actinides, rigorous classification of benzyl hapticity has been primarily performed using a method developed by Andersen, Zalkin, and co-workers (AZ model).<sup>4,11,27</sup> This model involves analyzing crystallographically characterized benzyl derivatives with a focus on trends involving the M–C distances to the phenyl group, specifically M–CH<sub>2</sub>, M–C<sub>ipso</sub>, and M–C<sub>ortho</sub> (M–C<sub>o</sub>) distances (Figure 2). These varying classification methods for different metals from across the periodic table suggest a certain degree of subjectivity in hapticity assignments for

benzyl complexes overall. A compilation of data for a variety of compounds can be found in Tables S1 and S2.

For a bonding interaction greater than  $\eta^1$  to be present, M–C bond distances should be within the sum of the van der Waals radii as previously noted.<sup>28,29</sup> Analysis of structurally characterized Th–C bonds in the Cambridge Structural Database (CSD) shows a range of 2.32–3.10 Å.<sup>24,30,31</sup> For the tetrabenzylthorium complexes reported here, all Th–C<sub>ipso</sub> and Th–C<sub>o</sub> distances are below 3.10 Å, thus suggesting multi-hapto interactions. It should be noted that meeting the distance criterion for a van der Waals interaction does *not necessarily* mean a hapto interaction is present, as there must also be electron density donated by the  $\pi$  system of the phenyl group to the metal ion, rather than just a weak electrostatic interaction with no significant orbital overlap.

A classic example is Cp\*<sup>2</sup>Th(Bn)<sub>3</sub>, reported by Marks and co-workers in 1982, where the authors describe that “the bond distances and angles are more in accord with a strong Th–C1 sigma interaction together with a more diffuse, unsymmetrical secondary interaction involving the (C<sub>2</sub>, C<sub>3</sub>, C<sub>7</sub>) part of the  $\pi$  system.” Marks and co-workers do mention secondary interactions with the adjacent carbons, but point out that the interactions are relatively weak: “the greater range of Th–C<sub>2</sub>, C<sub>3</sub>, C<sub>7</sub> contacts suggests that the potential-energy surface for the latter interaction is relatively flat”.

Hayton and co-workers originally reported  $[\text{K}(\text{THF})_2\text{[Th-(Bn)}_6]$ , made by the addition of 6 equiv of K(CH<sub>2</sub>Ph) to a THF solution of ThCl<sub>4</sub>(DME)<sub>2</sub>.<sup>5</sup> In this case, the thorium is in a “severely distorted octahedral geometry”, which the authors ascribe to the “multidentate” benzyl ligands. From structural parameters, the authors assign one of the groups as  $\eta^3$  hapticity, another group as  $\eta^2$  hapticity, and the rest as  $\eta^1$  hapticity. Further computational analysis predicts a distorted octahedral geometry but does not predict any multidentate behavior for any of the benzyl groups in  $[\text{K}(\text{THF})_2\text{[Th-(Bn)}_6]$ .

Andersen and Zalkin’s work established a different model for describing benzyl group hapticities in organoactinide species, the previously mentioned AZ model, where the following differences in bond distances are considered:  $\Delta = \delta_o - \delta_{ipso}$  and  $\Delta' = \delta_o' - \delta_{ipso}$ , where  $\delta_{ipso} = [\text{MC}_{ipso} - \text{MCH}_2]$ ,  $\delta_o = [\text{MC}_o - \text{CH}_2]$  and  $\delta_o' = [\text{MC}'_o - \text{MCH}_2]$ . MC<sub>o</sub> is the shorter metal-to-ortho carbon contact length, MC<sub>o'</sub> is the longer metal-to-ortho contact length, MCH<sub>2</sub> is the metal-to-methylene carbon bond length, and MC<sub>ipso</sub> is the metal-to-ipso carbon contact length. Here, a comparable magnitude between the  $\Delta$  and  $\Delta'$  parameters indicates a  $\eta^4$ -benzyl (about  $|\Delta' - \Delta| \leq 0.3$ ); for the previously published U(Bn)<sub>4</sub>, this was

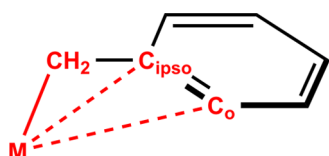


Figure 2. M–C distances for hapticity discussion in benzyl ligands.

**Table 2.** Hapticity Assignments of 1-THF, 2-dme, and 3-dmpe<sup>a</sup>

	angle	$\delta_{\text{ipso}}$	$\delta_{\text{o}}$	$\delta_{\text{o}'}$	$\Delta$	$\Delta'$	$ \Delta' - \Delta $	AZ model
<b>1-THF</b>								
C1	102.12	0.650	1.234	1.429	0.584	0.779	0.20	$\eta^4$
C8	123.34	1.027	1.776	1.835	0.749	0.808	0.06	$\eta^4$
C15	94.41	0.479	0.997	1.191	0.518	0.712	0.19	$\eta^4$
C22	87.24	0.327	0.717	1.041	0.390	0.714	0.32	$\eta^3$
<b>2-dme</b>								
C1A	114.01	0.861	1.581	1.647	0.720	0.786	0.07	$\eta^4$
C8A	100.77	0.623	1.018	1.539	0.395	0.916	0.52	$\eta^3$
C15A	99.73	0.599	1.041	1.467	0.442	0.868	0.43	$\eta^3$
C22A	85.47	0.277	0.712	0.901	0.435	0.624	0.19	$\eta^4$
<b>2-dme</b>								
C1B	116.52	0.925	1.545	1.761	0.620	0.836	0.22	$\eta^4$
C8B	108.00	0.770	1.206	1.707	0.436	0.937	0.50	$\eta^3$
C15B	116.52	0.542	0.885	1.431	0.343	0.889	0.55	$\eta^3$
C22B	88.25	0.348	0.884	0.902	0.536	0.554	0.02	$\eta^4$
<b>3-dmpe</b>								
C1	105.73	0.715	1.291	1.525	0.576	0.810	0.23	$\eta^4$
C8	99.71	0.597	1.154	1.349	0.557	0.752	0.20	$\eta^4$
C15	111.86	0.841	1.511	1.627	0.670	0.786	0.12	$\eta^4$
C22	86.36	0.309	0.667	1.011	0.358	0.702	0.34	$\eta^3$

<sup>a</sup>  $\Delta = \delta_{\text{o}} - \delta_{\text{ipso}}$  and  $\Delta' = \delta_{\text{o}'} - \delta_{\text{ipso}}$ , where  $\delta_{\text{ipso}} = [\text{MC}_{\text{ipso}} - \text{MCH}_2]$ ,  $\delta_{\text{o}} = [\text{MC}_{\text{o}} - \text{CH}_2]$  and  $\delta_{\text{o}'} = [\text{MC}_{\text{o}'} - \text{MCH}_2]$ .

**Table 3.** Hapticity Assignments of 4- $\eta^3$  and 4- $\eta^4$ 

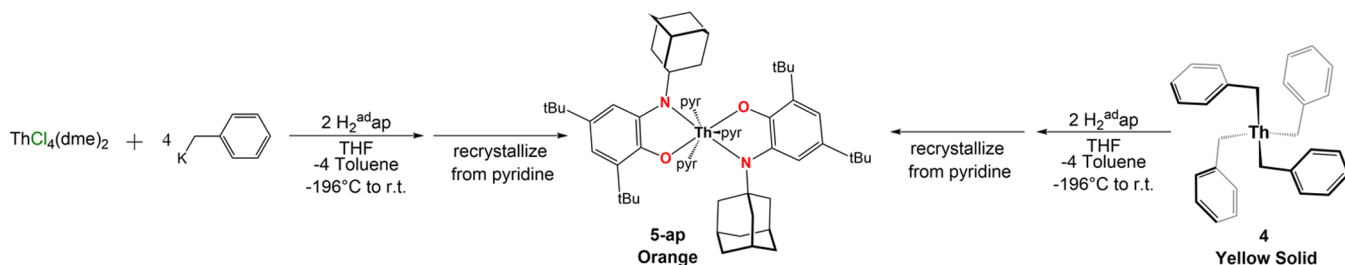
	angle	$\delta_{\text{ipso}}$	$\delta_{\text{o}}$	$\delta_{\text{o}'}$	$\Delta$	$\Delta'$	$ \Delta' - \Delta $	AZ model
<b>4-<math>\eta^4</math></b>								
C1	85.36	0.283	0.740	0.865	0.457	0.582	0.13	$\eta^4$
C8	85.14	0.276	0.676	0.896	0.400	0.620	0.22	$\eta^4$
C15	88.90	0.368	0.898	0.967	0.530	0.599	0.07	$\eta^4$
C22	82.53	0.215	0.634	0.758	0.419	0.543	0.12	$\eta^4$
<b>4-<math>\eta^3</math> (190 K)</b>								
C1	86.49	0.311	0.655	1.019	0.344	0.708	0.36	$\eta^3$
C8	86.95	0.318	0.684	1.009	0.366	0.691	0.33	$\eta^3$
C15	88.51	0.358	0.614	1.234	0.256	0.876	0.62	$\eta^3$
C22	86.48	0.313	0.611	1.082	0.298	0.769	0.47	$\eta^3$
<b>4-<math>\eta^3</math> (150 K)</b>								
C1A	85.97	0.302	0.600	1.075	0.298	0.773	0.48	$\eta^3$
C8A	87.17	0.321	0.670	1.067	0.349	0.746	0.40	$\eta^3$
C15A	86.01	0.295	0.638	1.014	0.343	0.719	0.38	$\eta^3$
C22A	86.26	0.308	0.614	1.149	0.306	0.841	0.54	$\eta^3$
<b>4-<math>\eta^3</math> (150 K)</b>								
C1B	86.06	0.297	0.611	1.256	0.314	0.959	0.65	$\eta^3$
C8B	86.92	0.317	0.627	1.100	0.310	0.783	0.47	$\eta^3$
C15B	86.68	0.319	0.643	1.011	0.324	0.692	0.37	$\eta^3$
C22B	85.45	0.303	0.695	1.014	0.392	0.711	0.32	$\eta^3$

the case.<sup>4</sup> A large difference of approximately  $|\Delta' - \Delta| > 0.3$  was used to indicate an  $\eta^3$ -benzyl, as this difference is consistent with  $\eta^3$  classification from previous work.<sup>4,5,11</sup> The limitations of this model include that only  $\eta^3$  and  $\eta^4$  interactions can be assigned;  $\eta^1$  and  $\eta^2$  interactions cannot be established. Furthermore, the AZ model does not consider the  $\text{M}-\text{CH}_2-\text{C}_{\text{ipso}}$  bond angle, which is used in discussions of hapticity involving transition metals and in some other actinide and lanthanide benzyl complexes.<sup>5,17,26,32</sup>

For the new tetrabenzylthorium derivatives reported here, their structural parameters, as well as the  $|\Delta' - \Delta|$  value and hapticity assignment according to the AZ model are summarized in Tables 2 and 3. In the cases of 1-THF, 2-dme, and 3-dmpe, some clear trends emerge when looking at

the  $|\Delta' - \Delta|$  value. When this value is above 0.3 Å, as indicated in the tables, the assignment given is a  $\eta^3$  benzyl, in concert with the original Andersen work. When the value is below 0.3 Å, an  $\eta^4$  benzyl is a more accurate description. For 1-THF, the two ancillary THF ligands are more flexible than the chelating dme ligand in 2-dme; therefore, there are three  $\eta^4$  benzenes according to this model. Both molecules in the unit cell only have two  $\eta^4$  benzenes, which could be due to crystal packing or the bidentate nature of the dme ligand, which prevents additional coordination. In the case of dmpe,  $\eta^4$  benzyl interactions are likely due to the fact that the Th-P bond distance is longer than the Th-O bond distance, creating a sterically less encumbered Th center where the benzenes have a closer approach.

Scheme 3. Synthesis of 5-ap



With the hapticities established based on the AZ models, it is also important to look at the angles, which have not been taken into account in the original model. Based on the assigned hapticities, it is possible to see that for the groups assigned as  $\eta^3$  benzylics, the  $\text{Th}-\text{CH}_2-\text{C}_{\text{ipso}}$  angle is typically less than 90°. For those benzylics assigned as  $\eta^4$ , the angle is generally above 90°. Therefore, the sharper the angle, the less the interaction with the thorium ion, resulting in a smaller hapticity. This is because the sharper the  $\text{Th}-\text{CH}_2-\text{C}_{\text{ipso}}$  angle is, the more twisted the benzyl is, resulting in a lesser interaction with the ortho carbons, which in turn generates a larger  $\Delta'$ .

In the absence of the ancillary ligands, compounds 4 have  $|\Delta' - \Delta|$  values that vary from 0.07 to 0.62. The benzyl groups that are above 0.3 fit are again assigned to an  $\eta^3$  hapticity, **4- $\eta^3$** , whereas those with values lower than that are assigned to  $\eta^4$  benzylics, **4- $\eta^4$** . Therefore, the assignments are different depending on the polymorph. Unlike in the cases of **1-THF**, **2-dme**, and **3-dmpe**, there is not a clear trend here for the  $\text{Th}-\text{CH}_2-\text{C}_{\text{ipso}}$  angle, as all angles are below 90° for this subset of compounds; no correlation can be made in these cases between angle and benzyl group hapticity.

**Synthesis of Thorium bis(amidophenolate) Complex, 5-ap, from 1-THF/ 2-dme and 4.** Despite tetrabenzylthorium having been discovered in 1974, it has not been routinely used as a synthon for organothorium derivatives. This is likely due to the instability of the complex during isolation; however, we hypothesize that it can still be produced *in situ* to be useful for synthesis. To test this, a thorium amidophenolate compound was synthesized such that it could be compared with previously published work by our group and to obtain preliminary reactivity insights.<sup>33–35</sup>

Compounds **1-THF** and **2-dme** were first synthesized *in situ* as previously described and immediately after, a cold THF solution of 2 equiv  $\text{H}_2^{\text{adap}}$  was added. Upon workup, a pale-yellow powder was obtained (Scheme 3) and assigned as  $\text{Th}(\text{adap})_2(\text{THF})_x$ . Unfortunately,  $\text{Th}(\text{adap})_2(\text{THF})_x$  could not be isolated from unreacted ligand due to solubility issues. Using a more basic solvent, pyridine, and recrystallizing allowed isolation of  $\text{Th}(\text{adap})_2(\text{pyr})_3$ , **5-ap**, in low yields (15%). The low yield was due to the partial conversion of  $\text{Th}(\text{adap})_2(\text{THF})_x$  to  $\text{Th}(\text{adap})_2(\text{pyr})_3$  when pyridine was added. Despite the low yield, the pyridine adduct was convenient to work with for crystallization. These procedures were repeated with isolated tetrabenzylthorium, **4**, and **5-ap** was obtained in similar yield. Performing this reaction in noncoordinating solvents such as toluene did not produce a nonsolvated product with reasonable purity.

$^1\text{H}$  NMR spectroscopy of **5-ap** showed 10 resonances: three resonances were assigned to the adamantyl groups, three for the pyridines, two for the *tert*-butyl groups, and two for the aromatic hydrogens on the ligand (Figure S9). The  $^{13}\text{C}$  NMR

spectrum had the expected number of resonances assigned to pyridine, aromatic ligand carbons, adamantyl, and *tert*-butyl groups (Figure S10). IR spectroscopy was also performed, with no evidence for NH absorption bands, consistent with full deprotonation of  $\text{H}_2^{\text{adap}}$  ligands to form the metallated product from tetrabenzylthorium (Figure S11).

X-ray quality crystals of **5-ap** were grown from a concentrated pyridine solution layered with pentane (1:2 ratio) at  $-35\text{ }^{\circ}\text{C}$  (Figure 3). Refinement of the data showed a

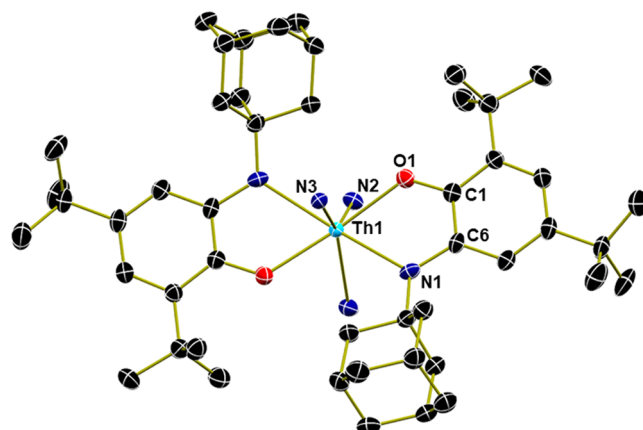


Figure 3. Molecular structure of **5-ap** shown with 30% probability ellipsoids. Hydrogen atoms, pyridine carbons, and co-crystallized solvent molecules are omitted for clarity.

seven-coordinate thorium center, with two amidophenolate ligands and three pyridine ligands. The  $\text{Th}-\text{O}$  and  $\text{Th}-\text{N}$  bond lengths are similar to those of previously published amidophenolate complexes (Figure S8).<sup>33</sup> The  $\text{C}-\text{O}$  and  $\text{C}-\text{N}$  bond lengths differ slightly but are within the expected range for single bonds.<sup>30,36–38</sup> Compared with the analogous uranium structure, the only major difference is that there are three solvent molecules on **5-ap** while there are only two for the uranium complex. The isolation of the **5-ap** complex shows the utility of tetrabenzylthorium as a synthon for ligand metalation.

## CONCLUSIONS

In summary, an updated synthesis and the first molecular structure of ancillary ligand-free tetrabenzylthorium (i.e.,  $\text{Th}(\text{Bn})_4$ , **4**), which was initially synthesized in 1974 by Thiele and co-workers, is reported here. The synthesis of analogous Lewis base compounds, **1-THF** and **2-dme**, is also reported along with an updated molecular structure of **3-dmpe**. These complexes were characterized by  $^1\text{H}$  NMR spectroscopy and X-ray crystallography to get a full picture of their solution and solid-state behaviors. Finally, the synthesis of an amidopheno-

late complex, **5-ap**, was explored with **4** *in situ* and isolated to understand the utility of tetrabenzylthorium as a starting material for the generation of other organothorium complexes.

The ancillary ligand-free compound, **4**, is a final entry to a family of tetravalent homoleptic benzyl species containing titanium, zirconium, hafnium, and uranium. Thorium is the largest of these ions and thus has more degrees of freedom in its coordination mode compared to its smaller counterparts. Based on the previous bonding model established by Andersen and co-workers, the benzyl groups in the cases shown here fit nicely with that work, establishing these groups as either  $\eta^3$  or  $\eta^4$  benzyls. Future studies will focus on understanding fundamental organometallic reactions with these species.

## ASSOCIATED CONTENT

### Supporting Information

The Supporting Information is available free of charge at <https://pubs.acs.org/doi/10.1021/acs.organomet.3c00248>.

NMR, IR, UV-vis, magnetic, and crystallographic data.  
CCDC 2214584–2214590 (PDF)

### Accession Codes

CCDC 2214584–2214590 contain the supplementary crystallographic data for this paper. These data can be obtained free of charge via [www.ccdc.cam.ac.uk/data\\_request/cif](http://www.ccdc.cam.ac.uk/data_request/cif), or by emailing [data\\_request@ccdc.cam.ac.uk](mailto:data_request@ccdc.cam.ac.uk), or by contacting The Cambridge Crystallographic Data Centre, 12 Union Road, Cambridge CB2 1EZ, UK; fax: +44 1223 336033.

## AUTHOR INFORMATION

### Corresponding Author

Suzanne C. Bart – *H. C. Brown Laboratory, Department of Chemistry, Purdue University, West Lafayette, Indiana 47907, United States*;  [orcid.org/0000-0002-8918-9051](https://orcid.org/0000-0002-8918-9051); Email: [sbart@purdue.edu](mailto:sbart@purdue.edu)

### Authors

D. M. Ramitha Y. P. Rupasinghe – *H. C. Brown Laboratory, Department of Chemistry, Purdue University, West Lafayette, Indiana 47907, United States*

Makayla R. Baxter – *H. C. Brown Laboratory, Department of Chemistry, Purdue University, West Lafayette, Indiana 47907, United States*

Matthias Zeller – *H. C. Brown Laboratory, Department of Chemistry, Purdue University, West Lafayette, Indiana 47907, United States*;  [orcid.org/0000-0002-3305-852X](https://orcid.org/0000-0002-3305-852X)

Complete contact information is available at:  
<https://pubs.acs.org/doi/10.1021/acs.organomet.3c00248>

### Notes

The authors declare no competing financial interest.

## ACKNOWLEDGMENTS

This material is based upon work supported by a grant from the National Science Foundation (CHE-1665170, grant to S.C.B.).

## REFERENCES

- Gilman, H.; Jones, R. G.; Bindschadler, E.; Blume, D.; Karmas, G.; Martin, G. A.; Nobis, J. F.; Thirtle, J. R.; Yale, H. L.; Yoeman, F. A. *Organic Compounds of Uranium. I. 1,3-Dicarbonyl Chelates*. *J. Am. Chem. Soc.* **1956**, *78*, 2790–2792.
- Köhler, E.; Brüser, W.; Thiele, K. H. Untersuchungen über benzylübergangsmetallverbindungen: III. Darstellung und eigenschaften des tetrabenzylthoriums. *J. Organomet. Chem.* **1974**, *76*, 235–240.
- Thiele, K. H.; Opitz, R.; Köhler, E. Beiträge zur Chemie der Alkylverbindungen von Übergangsmetallen. XXIV. Darstellung und Eigenschaften von Tetrabenzylmolybdän und -uran. *Z. Anorg. Allg. Chem.* **1977**, *435*, 45–48.
- Kraft, S. J.; Fanwick, P. E.; Bart, S. C. Carbon–Carbon Reductive Elimination from Homoleptic Uranium(IV) Alkyls Induced by Redox-Active Ligands. *J. Am. Chem. Soc.* **2012**, *134*, 6160–6168.
- Seaman, L. A.; Walensky, J. R.; Wu, G.; Hayton, T. W. In Pursuit of Homoleptic Actinide Alkyl Complexes. *Inorg. Chem.* **2013**, *52*, 3556–3564.
- Chen, R.; Qin, G.; Li, S.; Edwards, A. J.; Piltz, R. O.; Del Rosal, I.; Maron, L.; Cui, D.; Cheng, J. Molecular Thorium Trihydrido Clusters Stabilized by Cyclopentadienyl Ligands. *Angew. Chem., Int. Ed.* **2020**, *59*, 11250–11255.
- Pool, J. A.; Scott, B. L.; Kiplinger, J. L. A New Mode of Reactivity for Pyridine N-Oxide: C–H Activation with Uranium(IV) and Thorium(IV) Bis(alkyl) Complexes. *J. Am. Chem. Soc.* **2005**, *127*, 1338–1339.
- Button, Z. E.; Higgins, J. A.; Suvova, M.; Cloke, F. G. N.; Roe, S. M. Mixed sandwich thorium complexes incorporating bis(triisopropylsilyl)cyclooctatetraenyl and pentamethylcyclopentadienyl ligands: synthesis, structure and reactivity. *Dalton Trans.* **2015**, *44*, 2588–2596.
- Fortier, S.; Melot, B. C.; Wu, G.; Hayton, T. W. Homoleptic Uranium(IV) Alkyl Complexes: Synthesis and Characterization. *J. Am. Chem. Soc.* **2009**, *131*, 15512–15521.
- Sears, J. D.; Sergent, D.-C.; Baker, T. M.; Brennessel, W. W.; Autschbach, J.; Neidig, M. L. The Exceptional Diversity of Homoleptic Uranium–Methyl Complexes. *Angew. Chem., Int. Ed.* **2020**, *59*, 13586–13590.
- Edwards, P. G.; Andersen, R. A.; Zalkin, A. Preparation of tetraalkyl phosphine complexes of the f-block metals. Crystal structure of  $\text{Th}(\text{CH}_2\text{Ph})_4(\text{Me}_2\text{PCH}_2\text{CH}_2\text{PMe}_2)$  and  $\text{U}(\text{CH}_2\text{Ph})_3\text{Me}(\text{Me}_2\text{PCH}_2\text{CH}_2\text{PMe}_2)$ . *Organometallics* **1984**, *3*, 293–298.
- Lauke, H.; Swepton, P. J.; Marks, T. J. Synthesis and characterization of a homoleptic actinide alkyl. The heptamethylthorate(IV) ion: a complex with seven metal–carbon–sigma bonds. *J. Am. Chem. Soc.* **1984**, *106*, 6841–6843.
- Matsui, S.; Yoshida, Y.; Takagi, Y.; Spaniol, T. P.; Okuda, J. Pyrrolide-imine benzyl complexes of zirconium and hafnium: synthesis, structures, and efficient ethylene polymerization catalysis. *J. Organomet. Chem.* **2004**, *689*, 1155–1164.
- Noor, A.; Kretschmer, W. P.; Glatz, G.; Meetsma, A.; Kempe, R. Synthesis and Structure of Zirconium and Hafnium Polymerisation Catalysts Stabilised by Very Bulky Aminopyridinato Ligands. *Eur. J. Inorg. Chem.* **2008**, *2008*, 5088–5098.
- Chien, J. C. W.; Salajka, Z. Syndiospecific polymerization of styrene. I. Tetrabenzyl titanium/methylaluminoxane catalyst. *J. Polym. Sci., Part A: Polym. Chem.* **1991**, *29*, 1243–1251.
- Chen, C.; Lee, H.; Jordan, R. F. Synthesis, Structures, and Ethylene Polymerization Behavior of Bis(pyrazolyl)borate Zirconium and Hafnium Benzyl Complexes. *Organometallics* **2010**, *29*, 5373–5381.
- Rong, Y.; Al-Harbi, A.; Parkin, G. Highly Variable  $\text{Zr}-\text{CH}_2-\text{Ph}$  Bond Angles in Tetrabenzylzirconium: Analysis of Benzyl Ligand Coordination Modes. *Organometallics* **2012**, *31*, 8208–8217.
- Davies, G. R.; Jarvis, J. A. J.; Kilbourn, B. T. The crystal and molecular structures (at  $-40\text{ }^\circ\text{C}$ ) of the tetrabenzyls of titanium, hafnium, and tin. *J. Chem. Soc. D* **1971**, 1511–1512.
- Garner, M. E.; Parker, B. F.; Hohloch, S.; Bergman, R. G.; Arnold, J. Thorium Metallacycle Facilitates Catalytic Alkyne Hydrophosphination. *J. Am. Chem. Soc.* **2017**, *139*, 12935–12938.
- Suvova, M.; O'Brien, K. T. P.; Farnaby, J. H.; Love, J. B.; Kaltsoyannis, N.; Arnold, P. L. Thorium(IV) and Uranium(IV) trans-Calix[2]benzene[2]pyrrolide Alkyl and Alkynyl Complexes: Syn-

thesis, Reactivity, and Electronic Structure. *Organometallics* **2017**, *36*, 4669–4681.

(21) Gardner, B. M.; Cleaves, P. A.; Kefalidis, C. E.; Fang, J.; Maron, L.; Lewis, W.; Blake, A. J.; Liddle, S. T. The role of 5f-orbital participation in unexpected inversion of the  $\sigma$ -bond metathesis reactivity trend of triamidoamine thorium(IV) and uranium(IV) alkyls. *Chem. Sci.* **2014**, *5*, 2489–2497.

(22) Cruz, C. A.; Emslie, D. J. H.; Harrington, L. E.; Britten, J. F. Single and Double Alkyl Abstraction from a Bis(anilido)xanthene Thorium(IV) Dibenzyl Complex: Isolation of an Organothorium Cation and a Thorium Dication. *Organometallics* **2008**, *27*, 15–17.

(23) Qin, G.; Wang, Y.; Shi, X.; Del Rosal, I.; Maron, L.; Cheng, J. Monomeric thorium dihydrido complexes: versatile precursors to actinide metallacycles. *Chem. Commun.* **2019**, *55*, 8560–8563.

(24) Bruno, I. J.; Cole, J. C.; Edgington, P. R.; Kessler, M.; Macrae, C. F.; McCabe, P.; Pearson, J.; Taylor, R. New software for searching the Cambridge Structural Database and visualizing crystal structures. *Acta Cryst. B* **2002**, *58*, 389–397.

(25) Cotton, F. A. Proposed nomenclature for olefin-metal and other organometallic complexes. *J. Am. Chem. Soc.* **1968**, *90*, 6230–6232.

(26) Woole, A. J.; Mills, D. P.; Lewis, W.; Blake, A. J.; Liddle, S. T. Lanthanide tri-benzyl complexes: structural variations and useful precursors to phosphorus-stabilised lanthanide carbenes. *Dalton Trans.* **2010**, *39*, 500–510.

(27) Zalkin, A.; Brennan, J. G.; Andersen, R. A. Dibenzyl[1,2-bis(dimethylphosphino)ethane]bis(cyclopentadienyl)thorium(IV). *Acta Cryst. C* **1987**, *43*, 421–423.

(28) Dvorak, M. A.; Ford, R. S.; Suenram, R. D.; Lovas, F. J.; Leopold, K. R. van der Waals vs. covalent bonding: microwave characterization of a structurally intermediate case. *J. Am. Chem. Soc.* **1992**, *114*, 108–115.

(29) Pauling, L. The Nature of the Chemical Bond. Application of Results Obtained from the Quantum Mechanics and from a Theory of Paramagnetic Susceptibility to the Structure of Molecules. *J. Am. Chem. Soc.* **1931**, *53*, 1367–1400.

(30) Yang, P.; Zhou, E.; Hou, G.; Zi, G.; Ding, W.; Walter, M. D. Experimental and Computational Studies on the Formation of Thorium–Copper Heterobimetallics. *Chem. Eur. J.* **2016**, *22*, 13845–13849.

(31) Zhang, C.; Yang, P.; Zhou, E.; Deng, X.; Zi, G.; Walter, M. D. Reactivity of a Lewis Base Supported Thorium Terminal Imido Metallocene toward Small Organic Molecules. *Organometallics* **2017**, *36*, 4525–4538.

(32) Wasilke, J.-C.; Ziller, J. W.; Bazan, G. C. Trimethylphosphine-bis(benzyl)nickel: Synthesis and Characterization. *Adv. Synth. Catal.* **2005**, *347*, 405–408.

(33) Rupasinghe, D. M. R. Y. P.; Gupta, H.; Baxter, M. R.; Higgins, R. F.; Zeller, M.; Schelter, E. J.; Bart, S. C. Elucidation of Thorium Redox-Active Ligand Complexes: Evidence for a Thorium-Tri-radical Species. *Inorg. Chem.* **2021**, *60*, 14302–14309.

(34) Matson, E. M.; Opperwall, S. R.; Fanwick, P. E.; Bart, S. C. “Oxidative Addition” of Halogens to Uranium(IV) Bis(amidophenolate) Complexes. *Inorg. Chem.* **2013**, *52*, 7295–7304.

(35) Rupasinghe, D. M. R. Y. P.; Baxter, M. R.; Gupta, H.; Poore, A. T.; Higgins, R. F.; Zeller, M.; Tian, S.; Schelter, E. J.; Bart, S. C. Actinide–Oxygen Multiple Bonds from Air: Synthesis and Characterization of a Thorium Oxo Supported by Redox-Active Ligands. *J. Am. Chem. Soc.* **2022**, *144*, 17423–17431.

(36) Karmel, I. S. R.; Elkin, T.; Fridman, N.; Eisen, M. S. Dimethylsilyl bis(amidinate)actinide complexes: synthesis and reactivity towards oxygen containing substrates. *Dalton Trans.* **2014**, *43*, 11376–11387.

(37) Zhang, C.; Hou, G.; Zi, G.; Ding, W.; Walter, M. D. An Alkali-Metal Halide-Bridged Actinide Phosphinidiide Complex. *Inorg. Chem.* **2019**, *58*, 1571–1590.

(38) Allen, F. H.; Kennard, O.; Watson, D. G.; Brammer, L.; Orpen, A. G.; Taylor, R. Tables of bond lengths determined by X-ray and neutron diffraction. Part 1. Bond lengths in organic compounds. *J. Chem. Soc., Perkin Trans. 2* **1987**, S1–S19.